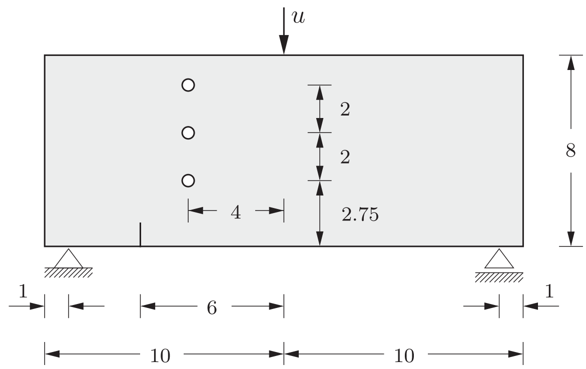

Figure 21. Asymmetric notched three-point bending test. Geometry, loading and boundary conditions from Bittencourt *et al.* [28]. The three holes have a diameter of 0.5.

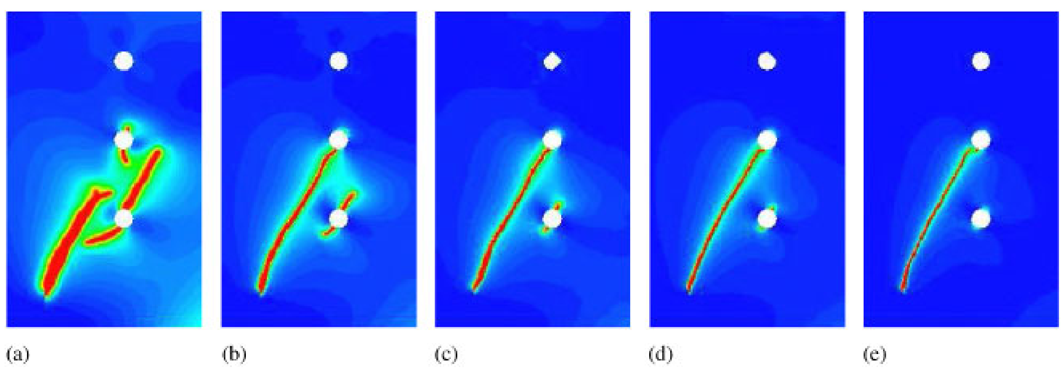

Figure 22. Asymmetric notched three-point bending test. Crack topology of the viscous three-field formulation (63) for different discretizations and corresponding length-scale parameters: (a) 20 000 elements with $l=0.15\,\text{mm}$; (b) 25 000 elements with $l=0.05\,\text{mm}$; (c) 35 000 elements with $l=0.035\,\text{mm}$; (d) 58 000 elements with $l=0.025\,\text{mm}$; and (e) 79 000 elements with $l=0.01\,\text{mm}$.

plots of the mesh with 79 000 elements. Again, blue and red colors correspond to the undamaged and the fully damaged, i.e. the cracked material, respectively.

6.5. Three-dimensional mode-I tension test

We now investigate the mode-I fracture problem of a three-dimensional tension test. The geometric setup of the problem and the boundary conditions are given in Figure 25(a). The same boundary value problem has been studied numerically by Miehe and Güerses [20]. We discretize a notched prismatic specimen with an unstructured mesh consisting of 60 675 linear tetrahedral elements. The mesh is refined in an area where the crack is expected to propagate in order to approximate the sharp limit case $l \to 0$. We apply the regularization parameter of $l=0.2\,\text{mm}$, which is approximatively twice times the element size to resolve the crack zone properly. The material parameters chosen are the bulk modulus $\lambda=12\,\text{kN/mm}^2$, the shear modulus $\mu=8\,\text{kN/mm}^2$ and the critical energy release rate $g_c=5\times10^{-4}\,\text{kN/mm}$. The boundary value problem is treated with the more robust three-field

DOI: 10.1002/nme